Josip Nižetić ✉
Pero Raos
Goran Šimunović
Miho Klaić
Alan Mutka

https://doi.org/10.21278/TOF.463039722
ISSN 1333-1124
eISSN 1849-1391

CALIBRATION OF A 5-AXIS CNC MACHINE FOR MAKING ORTHOSES BY MEANS OF A VISION SYSTEM

Summary

Orthoses are aids that compensate for the loss of function of a particular part of the locomotor system, while prostheses are devices that compensate for the loss of a part of the body. Digital technologies have enabled the measurement and the production of such aids. The production technology is a CNC or robotics arm-based system comprising several modules that are relatively positioned with a submillimetre precision. In practice, the implementation and calibration of such systems are challenging, especially in cases of adapting already used hardware or when the control unit is undocumented or closed to outside interventions. Our approach responds to several challenges, resulting in a unique visual solution for fast and affordable calibration. This approach enables reading the machine positions from an external computer without a physical connection to the control unit, tracking the movement of the machine in near real-time, and finally calculating calibration parameters of the observed system.

Key words: *computer vision, CNC, parallel kinematic, calibration, orthoses*

1. Introduction

Medical and technical professionals in orthotics and prosthetics (O&P) [1-3] deal with the production of orthoses (Fig. 1).

Making orthoses is a complex procedure that involves many professional staff [4] and is often uncomfortable for the patient. It takes a great deal of time and materials, and requires special tools. These facts are particularly true in the standard (manual) procedure. Although more or less specialised digital production solutions are available on the market, a manual approach is still predominant in most orthotic laboratories for the production of moulds for orthoses. In recent times, the use of digital acquisition, digital technologies, and digital manufacturing methods has increased, but their inaccessibility and high level of complexity mean that they are often unprofitable [5,6]. Making a custom-made orthosis involves defining the surface area of the body part to which the orthosis will be applied, the function of which will be modified by the orthosis. In the standard (manual) procedure, this volumetric measurement involves shaping a softer material on the part of the body for which the orthosis

is to be made. After the impression is formed by solidification, a shape (a negative mould) is obtained. After subsequent procedures, a positive mould is obtained, on the basis of which an orthosis is formed by the thermoforming of the material. A digital solution that describes the shape of the surface of the body part of interest involves digitalisation using a 3D digitising device [7,8].

Fig. 1 Orthoses

Today, we can find numerous commercial forms of 3D digitising devices. They are primarily general-purpose and can be used, with or without modifications, to scan body parts. In orthotics, there is a need for specific solutions because of the following specific problems:

- there is a need for rapid acquisition;
- the imaging area is often large;
- the object is not entirely static, and it must usually be in a forced position during scanning; and
- the patient may be traumatised and often cannot speak.

By resolving these problems, it is possible to implement the scanning process quickly and easily with reasonable accuracy. Also, the results of the process are in a form that can be easily imported into any CAD program.

Once the result has been imported, the surface is modified to create a model, based on which a mould (positive) (Fig. 2), or the orthosis itself, is made using an appropriate production technology. High production costs are among the major obstacles to a wider practical use of CAD/CAM technology [9]. Initial investments in production technology (e.g. CNC milling machines and lathes, and robotic arms) are substantial, especially when it comes to new equipment [10,11].

The calibration and implementation of orthoses can be accelerated by the application of an appropriate computer vision system. With such a vision system, it is possible to define the geometry of the machine, the work envelope, and the precision of tasks, and to calibrate tools without the need to connect to the control system of the machine, which may be old or closed to external control.

A question that is often asked is how a machine that has already been used can be adapted for making orthoses. For the needs of orthotic practice, it is possible to modify the existing designs of production machines and robots. Given that softer polymeric materials are mainly

used in the production, and tolerances are tighter than those for metal machining, adaptation is often carried out on machines and robots that have already been used (for example, in the automotive industry). Despite showing signs of wear, such units still have satisfactory technical characteristics for use in the manufacture of orthoses. Their price and reliable technical capabilities make them a good choice, especially in small and medium-sized laboratories.

Fig. 2 Moulds for orthoses made using the CAD / CAM technology

In the practice of making orthoses, there is also a need for the machine to have a specific design, sometimes accompanied with more complex kinematics, so the calibration procedure for such a machine varies significantly from the usual procedures. There is a requirement to adapt the technical characteristics to specifics that include changes in work envelope, unique material clamping devices, and upgrades with additional axes. Such units often come from industrial settings without accompanying documentation or a description of their technical characteristics and with older operating systems and controls, which may be closed to external access. This creates a need for solutions that are as inexpensive as possible and a requirement for the calibration procedure and the commissioning to be simplified. The application of vision systems allows us to find practical solutions that can meet most of these needs.

2. Materials and methods

In our example, a 5-axis numerical machine intended for making orthoses was created (Fig. 3). The machine consists of two functional modules. The first is based on parallel kinematics in a PSS (prismatic–spherical– spherical) three-stage design, which enables the movement of a mobile platform with a spindle motor and a milling tool in the work envelope. The second module is a configuration with A and C axes that make it possible to rotate and tilt the work pieces. This type of numerical processing machine is not common in orthotic practice; production units based on parallel kinematics are more commonly used in rapid prototyping (RPT) versions. Nevertheless, the creation of the numerical machine and the construction of the prototype enabled the concept testing and examination of the advantages and disadvantages of this approach.

Given the requirement to simplify the use of such a machine in practice and the fact that its design is unconventional, there was a need to determine the methodology for its calibration. The use of a vision system for this purpose was considered to be a possible approach.

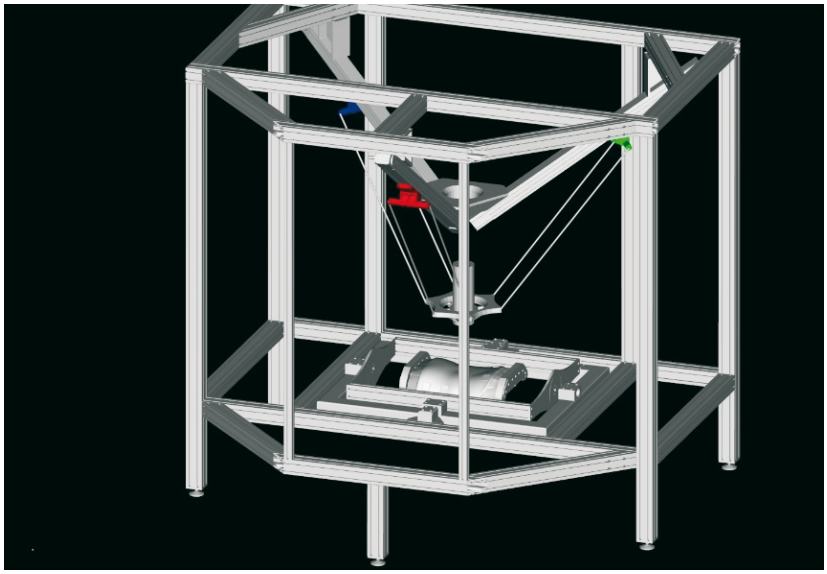

Fig. 3 A 5-axis orthosis machine based on parallel kinematics

The main problems that need to be solved by applying a vision system are:

- Reading the linear axis position values from an isolated control system;
- Defining the coordinate system (CS) and the work envelope of the machine and establishing a relationship with the CS of the vision system; and
- Calibrating the zero point and the A and C rotary axes.

The initial state was accompanied by the conditions listed below that significantly increased the complexity of the use of this procedure:

- Prototype of a CNC machine with an unconventional design;
- Tool movements realised on the principle of parallel kinematics; and
- Closed control system from which it is not possible to read positions from the encoder on the linear axes.

In addition to the problems listed above, the vision system for the calibration of the machine required features that would include:

- Spatial monitoring of the movement of the top of the calibration object in the form of a tentacle with infrared (IR) reflective beads;
- Tracking of fixed indexed markers in the machine work envelope;
- Monitoring of the positions of calibration objects fixed to the A and C axes of the machine;
- Visual reading of positions from the control computer display;
- Software module for communication and camera shooting, as well as for capturing and monitoring of markers in near real-time; and
- Vision software, including modules for capture management, calibration, reconstruction, optical capture recognition (OCR) [12-14], and a graphical interface.

In this research and research-related tasks, we used commercially available components of hardware. The only major exception was the use of the Optitrack vision tracking system [15], which was used for robustness and accuracy to confirm the principles, while the final project will include the use of more affordable vision components. This approach to the problem simplified the realisation of the system and its use in practice. Since the components used are widely available, they can be easily acquired and quickly replaced when needed. It is possible

to replace them with components that are different from those initially used because this is permitted by the technical design and the practical and flexible calibration procedure.

The hardware used in the realisation of our vision solution includes:

- Camera to record the screen of the control unit. This camera is connected by means of Bluetooth or WLAN to the main processing PC;
- Vision system with two cameras (our set includes our own system defined by ourselves and a commercial Optitrack system);
- Disc with IR light-emitting diodes (LEDs) on the rim, placed around the camera lens to illuminate the scene;
- Calibration objects, which can be a probe, handles, and plates with IR markers in the form of circular labels and beads with IR reflective surface and augmented reality markers, i.e. ArUco markers . Flat plates with a binary pattern in the form of a chessboard are also used in this procedure; and
- Tripods, fixing plates, and cables.

2.1 Vision system calibration procedure

The calibration procedure is an indispensable condition for the application of any vision system when used as a measuring system. This procedure must be carried out precisely because the accuracy of all other measurements depends on the results obtained.

The primary calibration procedure for cameras includes finding intrinsic and extrinsic parameters and their interrelationship.

Precisely made calibration objects (plates) with coded binary patterns and known geometric characteristics are used for this procedure. In our approach, we used Zhang's method [16-18]. This involves capturing a planar calibration object (Fig. 4) with a chessboard pattern from multiple views.

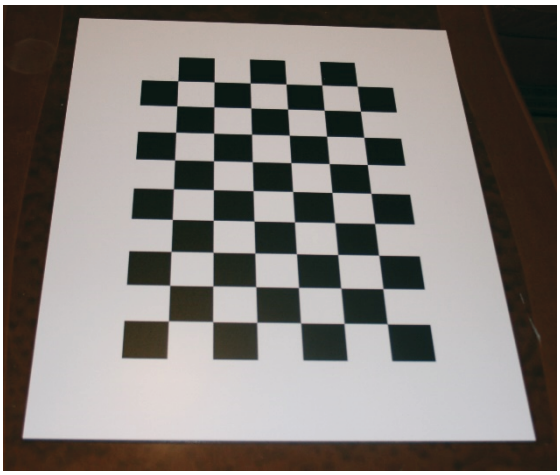

Fig. 4 Planar calibration object with a chessboard pattern

This method was chosen because it eliminates the need to create complex 3D calibration objects, it is easy to use, and it achieves high quality results. In addition, it allows the captured material to be used for the realisation of other steps s in the procedure, such as the calibration of the relative position of the camera.

The procedure of extracting and indexing significant points makes it possible to determine the homography between the model of the calibration of a planar object and its image from a single view. Initially, the position of the separated and indexed corners in 3D space is not known, but their position on the plate (the model, in its CS) is known. The points of the physical

object (the chessboard) have the Z coordinate equal to 0, and the X and Y positions of the separated indexed corners in relation to the physical dimensions of the board and its CS are known. Zhang's procedure involves obtaining intrinsic and extrinsic camera parameters.

2.1.1 Intrinsic parameters

The crucial segment in defining intrinsic parameters involves finding the calibration matrix $\boldsymbol{K}$ [19].

$$\boldsymbol{K} = \begin{bmatrix} \alpha & \gamma & ux \\ 0 & \beta & uy \\ 0 & 0 & 1 \end{bmatrix} \tag{1}$$

where α is the focal length for the x-axis, β is the focal length for the y axis, and γ is the skew factor. In the optical centre of the camera, ux is the centre of the camera along the x-axis, while vy is the centre of the camera along the y axis.

The values of ux and vy should be very close to the centre of the image (image width / 2, image height / 2) for cameras used for measurement. The ratio of the focal lengths α and β should ideally be 1.

The projection of the spatial point ($\boldsymbol{M}$) on the camera screen ($\mathbf{m}$) is achieved by the transformation (2):

$$s\mathbf{m}=\boldsymbol{K}[\boldsymbol{R}\ \mathbf{t}]\boldsymbol{M} \tag{2}$$

where s is scalar

$$s[u\ v\ 1]^T=\boldsymbol{K}[\mathbf{r}_1\ \mathbf{r}_2\ \mathbf{r}_3\ \mathbf{t}][X\ Y\ Z\ 1]^T \tag{3}$$

Since for all views Z = 0 for a planar object, expression (4) holds:

$$s[u\ v\ 1]^T=\boldsymbol{K}[\mathbf{r}_1\ \mathbf{r}_2\ \mathbf{0}\ \mathbf{t}][X\ Y\ 0\ 1]^T \tag{4}$$

We do not need the last column of the rotational matrix, so we get expression (5):

$$s[u\ v\ 1]^T=\boldsymbol{K}[\mathbf{r}_1\ \mathbf{r}_2\ \mathbf{t}][X\ Y\ 1]^T \tag{5}$$

$$\boldsymbol{H}=\boldsymbol{K}[\mathbf{r}_1\ \mathbf{r}_2\ \mathbf{t}] \tag{6}$$

where $\boldsymbol{H}$ represents the matrix of homography [20], a transformation that maps a 2D point from one plane to another. Any two images of the same planar object from different perspectives are connected by a homography. The homography matrix can be obtained from as many as four points (although the N-point approach is also used) and their correspondent points in the second image. For the calibration of our vision system, the homography was determined between the corners on the calibration object (a planar object of known dimensions and positions, with a chessboard pattern) and their images.

$$s\mathbf{m}=\boldsymbol{H}\mathbf{M} \tag{7}$$

$$\boldsymbol{H}= [\mathbf{h}_1\ \mathbf{h}_2\ \mathbf{h}_3] \tag{8}$$

$$x'=\boldsymbol{H}x \tag{9}$$

$$[\mathbf{h}_1\ \mathbf{h}_2\ \mathbf{h}_3]=\lambda\boldsymbol{K}[\mathbf{r}_1\ \mathbf{r}_2\ \mathbf{t}] \tag{10}$$

λ is an arbitrary scalar

$$\mathbf{h}^T_1\boldsymbol{K}^T\boldsymbol{K}^{-1}\mathbf{h}_2=0 \tag{11}$$

$$\mathbf{h}^T_1\boldsymbol{K}^T\boldsymbol{K}^{-1}\mathbf{h}_1= \mathbf{h}^T_2\boldsymbol{K}^T\boldsymbol{K}^{-1}\mathbf{h}_2 \tag{12}$$

$\boldsymbol{K}^{-T}\boldsymbol{K}^{-1}$ is the image of an absolute conic (IAC ($\boldsymbol{\omega}$)); the image of an absolute conic (absolute conic Ω∞) (second-order curve) consists of points lying on a plane at infinity. The absolute conic is of particular interest because of its connection to the calibration matrix $\boldsymbol{K}$.

If we apply expression (2) to the point X (13) located on the absolute conic (Ω∞)

$$\boldsymbol{X} = \begin{bmatrix} \mathbf{d} \\ 0 \end{bmatrix} \tag{13}$$

then it follows that

$$\mathbf{x}=\boldsymbol{K}[\boldsymbol{R}\ \mathbf{t}] \leftrightarrow \mathbf{x}=\boldsymbol{K}[\boldsymbol{R}\ \mathbf{t}]\mathbf{d} \tag{14}$$

$$\mathbf{x}\boldsymbol{K}^{-1}= \boldsymbol{R}\mathbf{d} \leftrightarrow \mathbf{x}^{T}\boldsymbol{K}\boldsymbol{K}^{T}\mathbf{x} = \mathbf{d}^{T}\mathbf{d} = 0 \tag{15}$$

and the projection of the point X is on the conic (16)

$$(\boldsymbol{K}\boldsymbol{K}^{T})^{-1} = \boldsymbol{\omega} = \text{IAC} \tag{16}$$

$$\boldsymbol{\omega} = \boldsymbol{B} = \boldsymbol{K}^{-T}\boldsymbol{K}^{-1} \tag{17}$$

where $\boldsymbol{B}$ is the symmetric matrix.

The IAC dual is a dual image of absolute conic (DIAC ($\boldsymbol{\omega}$*). If the conic is not degenerate, its dual is a symmetric matrix, its inverse.

$$\boldsymbol{\omega}^*=\boldsymbol{K}\boldsymbol{K}^{T} \tag{18}$$

The following procedure yields the components of the matrix of intrinsic parameters:

$$\boldsymbol{B} = \begin{bmatrix} B_{11} & B_{12} & B_{13} \\ B_{21} & B_{22} & B_{23} \\ B_{31} & B_{32} & B_{33} \end{bmatrix} \tag{19}$$

$$\mathbf{h}^{T}_{i}\boldsymbol{B}\mathbf{h}_{j}=(\mathbf{v}^{T})_{ij}\mathbf{b} \tag{20}$$

$$\mathbf{b}= (B_{11}\ B_{12}\ B_{22}\ B_{13}\ B_{23}\ B_{33}) \tag{21}$$

$$\boldsymbol{V}\mathbf{b}=0 \tag{22}$$

$\boldsymbol{V}$ is the 2n × 6 matrix

$$\begin{bmatrix} v_{12}^{T} \\ (v_{11} - v_{22})^{T} \end{bmatrix} \boldsymbol{b} = 0 \tag{23}$$

$$v_{ij} = [h_{i1}h_{j1},\ h_{i1}h_{j2} + h_{i2}h_{j1},\ h_{i2}h_{j2},\ h_{i3}h_{j1} + h_{i1}h_{j3},\ h_{i3}h_{j2} + h_{i2}h_{j3},\ h_{i3}h_{j3}]^{T} \tag{24}$$

If n ≥ 3 (where n is the number of homographies, which is related to the number of images of the calibration object), then **b** (21) is the eigenvector of the lowest eigenvalue of $\boldsymbol{V}^{T}\boldsymbol{V}$, from which the symmetric matrix $\boldsymbol{B}$ can be created.

Using the Cholesky decomposition, any symmetric matrix can be decomposed into the product of a lower triangular matrix and its transposition. Thus, the $\boldsymbol{K}$ matrix can be calculated from the $\boldsymbol{B}$ matrix, knowing its relationship to the intrinsic parameters of the camera (17).

This procedure is also shown in expressions (25-30)

$$v_y = (B_{12}B_{13} - B_{11}B_{23})/(B_{11}B_{22} - B^2_{12}) \tag{25}$$

$$\lambda = B_{33} - [B^2_{13} + v_x(B_{12}B_{13} - B_{11}B_{23})]/B_{11} \tag{26}$$

$$\alpha = \sqrt{\lambda/B_{11}} \tag{27}$$

$$\beta = \sqrt{\lambda B_{11}/(B_{11}B_{22} - B^2{}_{12})} \tag{28}$$

$$\gamma = -B_{12}\alpha^2\beta/\lambda \tag{29}$$

$$u_x = \gamma v_y/\beta - B_{13}\alpha^2/\lambda \tag{30}$$

For the skew factor γ, we can assume that its value is 0 or negligibly small for most industrial cameras.

There is a particular procedure that includes the distortion coefficients of lenses [21]. In our case, high quality lenses with low distortion (<0.1%) were used; therefore to preserve other image features that may be changed by correcting the distortion, this procedure was not used.

2.1.2 Extrinsic parameters

The extrinsic parameters of the camera (relationship between the coordinate system of the camera and that of the calibration object) are calculated by the following procedure:

$$\mathbf{r_1} = \lambda \boldsymbol{K}^{-1}\mathbf{h_1} \tag{31}$$

$$\mathbf{r_2} = \lambda \boldsymbol{K}^{-1}\mathbf{h_2} \tag{32}$$

$$\mathbf{r_3} = \mathbf{r_1} \times \mathbf{r_2} \tag{33}$$

$$\mathbf{t} = \lambda \boldsymbol{K}^{-1}\mathbf{h_3} \tag{34}$$

$$\lambda = 1/||\boldsymbol{K}^{-1}\mathbf{h_1}|| = 1/||\boldsymbol{K}^{-1}\mathbf{h_2}|| \tag{35}$$

If λ satisfies the conditions of expression (35), then the vector **t** defines the actual translation of the origin of the calibration plate in the camera CS for a given homography.

$$\boldsymbol{Q} = [\mathbf{r_1}\ \mathbf{r_2}\ \mathbf{r_3}] \tag{36}$$

The rotational matrix $\boldsymbol{Q}$ obtained due to noise is not a real rotational matrix because, if it were, it would have to meet the condition $\boldsymbol{R}^T\boldsymbol{R}=\boldsymbol{I}$, that is, it would have to be orthonormal.

$$\boldsymbol{Q} = \boldsymbol{USV}^T \tag{37}$$

Therefore, the best approximation of the $\boldsymbol{R}$ matrix, for which the Frobenius norm of ($\boldsymbol{Q}$-$\boldsymbol{R}$) is minimal (min || $\boldsymbol{Q}$-$\boldsymbol{R}$ ||), is required for the obtained matrix.

$$\boldsymbol{R} = \boldsymbol{UV}^T \tag{38}$$

This procedure determines the intrinsic and extrinsic parameters of the camera, thus meeting the essential condition for the realisation of the monitoring assembly.

A further procedure involves finding the relationship between the cameras. To do this, the results obtained in the previous procedure are used. As the main approach, we chose a method based on the application of projection matrices. The projection matrix $\boldsymbol{P}$ [22,23] is a singular 3 x 4 matrix that is defined as:

$$\boldsymbol{P} = \boldsymbol{K}[\boldsymbol{R}\ \mathbf{t}] \tag{39}$$

This matrix is often applied in a range of computer vision algorithms. If there are no hardware changes (e.g. focusing, lens change, and lens addition) on the camera, the matrix $\boldsymbol{K}$ is defined and will not change. The matrix $\boldsymbol{R}$ and the vector **t** define the relationship between the camera and the coordinate system of the calibration object; they change with each change in the position of the camera with respect to that of the object.

Our approach of finding spatial positions of the corners on the calibration object is based on the Perspective-3-Point method (P3P Grunert method [24]) and Direct Linear Transform

(DLT) methods [25,26]. A prerequisite for our approach is that the camera is pre-calibrated to intrinsic parameters as this allows the calculation of the angles between the lines on which the observed points are located. Expression (40) defines the lines that connect a point in space and its projection on the image of a calibrated camera. These lines pass through the principal point of the camera.

$$\mathbf{v}=\boldsymbol{K}^{-1}\mathrm{p} \tag{40}$$

Here, **v** is the direction vector, which passes through the principal point and at which the point p is in the image with normalised coordinates. By permuting the corners of the calibration object (chessboard pattern), a field of triangles is realized. Their sides (physical distances on the physical model) must be of different lengths. For further calculation, only those combinations of triangles whose areas or angles are above a specified threshold were selected in order to obtain more reliable results; triangles with areas below the specified threshold and those with sharp angles give less reliable results because of lower angular resolution between the points in the image. All the cameras that perform capturing have to be calibrated and the capturing of the calibration objects (chessboards) has to be synchronised. After capturing, the filtering process highlights only those triplets of points (three non-collinear points that are the corners of each triangle) that are visible in all cameras and that meet the criteria stated above. Ultimately, we have sets of pairs of 3D points obtained by the P3P process and their 2D positions in the images of all cameras.

Our choice of method took us in the direction of defining a projection matrix for each view. The projection matrix of an individual camera was obtained by the DLT method from related 3D and 2D points. Since the capturing was synchronised for all cameras, 3D points (spatial points) and their 2D correspondents (points in the image) in all views were obtained from each position of the calibration object (chessboards) in space; this was done to calibrate the intrinsic parameters of the camera. Three-dimensional points of an object that lie in the same plane and that are seen from one view are not suitable for the DLT algorithm since it requires a set of nonplanar 3D points. This was achieved by combining the results obtained from several views, because there was no shift of the cameras in the given configuration. Thus, a cloud of nonplanar 3D points was created; the correspondences between them were obtained by the same procedure together with synchronised capturing on other cameras. Metric projection matrices [P] were calculated from the results achieved (pairs of 3D and 2D points). Since these matrices were found for each camera by simultaneously capturing the object in a fixed position, they store information about the relationship between the cameras and the calibration object in space.

The QR decomposition of the projection matrices yielded the rotation matrix $\boldsymbol{R}$ and the translation vector **t** of each camera with respect to the calibration object. Subsequently, transformations that describe the relationship between all the cameras were achieved from these results. The aim here was to obtain the position of the camera centre in the CS of the calibration object and to make it possible to reconstruct the spatial positions of the observed points. A fundamental matrix $\boldsymbol{F}$ was created from pairs of correspondent points between individual images that were captured from different views (other cameras in the setup) for the calibration of intrinsic parameters. The fundamental matrix [27-30] is a 3x3 matrix that establishes relationships between points in individual images from two views on which there are at least eight correspondent points. If x and x' are the correspondent points on two images, then the epipolar line is:

$$\mathrm{l}'=\boldsymbol{F}\mathrm{x} \tag{41}$$

On this line, the correspondent point of the point x, x', must be found in another (connected) image, for which the $\boldsymbol{F}$ matrix has been calculated.

Also, for all correspondent pairs of points x and x', condition (42)

$$x'^{T}\boldsymbol{F}x=0 \tag{42}$$

applies, which is extremely useful in verifying the applicability of the procedure.

In our study, this approach proved to be effective as the points we worked with were extracted from the remaining content of the scene. These were the corners of the binary patterns on the calibration object, or the position of the maximum (e.g., for markers in the form of IR reflective balls).

In this way, it is possible to establish correspondences between two images with a high level of reliability, regardless of the interrelationships between the cameras. For these reasons, other methods are used that show an unambiguous relationship between points in the scene captured from multiple views; examples are the use of invariants such as cross-ratio numbers and the fact that, despite the projective transformation, points on the line remain on the line.

By knowing the correspondent points (x, x') in the images, the spatial positions of the points are determined using the calculated projection matrices of the cameras ($\boldsymbol{P}$, $\boldsymbol{P}'$).

$$\boldsymbol{X}=f(x,x',\boldsymbol{P},\boldsymbol{P}') \text{ [27]} \tag{43}$$

This example is used for two views, and a similar procedure is used for determining the spatial positions of the points from three or more views.

By projecting the points (using projection matrices), it is possible to refine the extrinsic parameters using iterative optimisation methods [31] and to improve the accuracy and stability of the entire procedure significantly. A3D point transformed by the projection matrix should ideally be projected exactly to the position of the correspondent point in the image for the pin-hole model of the camera. From the calculated camera centres, the position of 3D points in the CS of the calibration object (in our case, a cloud of 3D points) is known, as well as their orientation and transformations between views.

2.2 Reading linear axis position values from an isolated control system

The literature lists several methods that can be used to supplement our approach, which is one of our future goals. So far, we have described the basic methodology on which most of other procedures in our approach are based. In our study, we used a set of industrial cameras with optics and an Optitrack system. The Optitrack system was used because of its technical features that allow for the implementation of 120 fps capture in the IR range. All the algorithms followed in the calibration procedure were developed. By using these visual solutions, the application of the vision system in solving the tasks related to machine calibration was made possible. To carry out the planned calibration of the machine using our approach, it was first necessary to get the values of positions from the three linear axes that form the driving part of the tripod module of the machine. The driving part is based on parallel kinematics; it realizes the movements of a mobile platform with a spindle motor and a tool. From the values of positions and from necessary additional parameters, the XYZ positions of the tool tip are displayed through the program module for direct kinematics. The version of the machine control unit used in our application (model NCT 201, manufacturer NCT Kft. [32]) only allows commands to be entered via the loaded file, while machine control via an external computer is not possible. It is also not possible to read the values of the positions of the linear or rotational axes via an external computer. In our version, the possibility of reading these values from the screen of the control computer was considered (Fig. 5). Taking into account these facts, a particular vision system was adopted for the calibration procedure as a solution to this problem. This vision system also entailed capturing the screen of the control computer of the machine. Having obtained the result, the OCR software on another computer extracted the content of an individual region in near real-time and converted it into numerical values suitable for further processing.

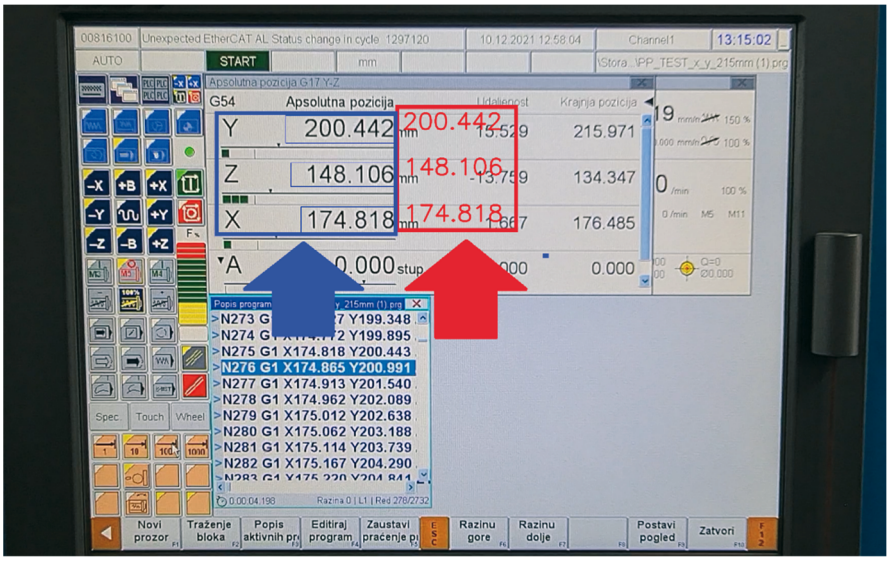

Fig. 5 Extraction of the values of the positions of machine linear axes using the OCR method. The textual content is extracted from the image content of the blue frame, and numerical values (red rectangle) are formed from it using the OCR method.

To increase the recognition success rate and reduce the error, we used a model optimised only for numbers. In our case, we used tesseract-ocr [33]. This is especially important because the screen contains content that cannot be accessed via the network and requires additional processing if it is to be displayed in XYZ coordinates. For example, the screen of a machine based on parallel kinematics shows the values of the positions of the linear axes, not the XYZ tool tip coordinates. Using this method, there was no need for different hardware solutions to connect to the control components of the machine.

This achievement solved the difficulties that had prevented the further implementation of the method; they are:

- It was not possible to connect to an external computer and read the values of the lever lengths (linear axes). Since the machine is tripod-based, the machine control screen displays the axis lengths L1, L2, and L3, without the XYZ tool tip position;
- It was not possible to control the machine via an external computer; and
- It was not possible to read other parameters of the machine such as the state of the input.

In addition to these problems in this version of the machine, the rotary axes (A and C) were not in the same plane, nor were they perpendicular to each other. After considering the existing conditions and options, a machine-based calibration procedure was proposed.

Our proposal for this procedure is outlined in the following three subsections:

2.2.1 Carrying out the necessary measurements using a vision system and calibration objects

A specially designed probe (tentacle) of known length and geometry was fixed in the tool holder of the machine tool (Fig. 6). The tentacle was made of aluminium, while its pointed tip was made of steel. When fixed, the tentacle axis and the motor spindle axis were collinear. The shaft of the tentacle is the part that was inserted into the collet. The central part of the tentacle was a flat surface, which was equidistantly shifted from the central axis by the radius of the spherical markers. On this surface, vision markers were placed in such a way that their centres were on the tentacle axis. There were four markers, with known mutual distances, which, in addition to defining the orientation and position of the tentacle tip, allowed their undoubted

indexing. In addition, the distances of each marker to the tip of the tool and to the opposite end (shaft), which was fixed in the collet during the procedure, were known. Another set of IR vision markers was placed on the mobile platform of the machine. The purpose of these markers was to monitor the movement of the mobile platform, and to optimise the generation of paths for the parallel kinematic module. There were six or more of these markers that were located in a plane passing through the centres of the spherical joints through which the mobile platform was connected by levers to the base platform. At the same time, three markers were placed on the assumed locations of the joints (since it is a tripod version) between the levers and the mobile platform. The machine is driven by three levers that are connected to linear axes (X, Y, and Z);

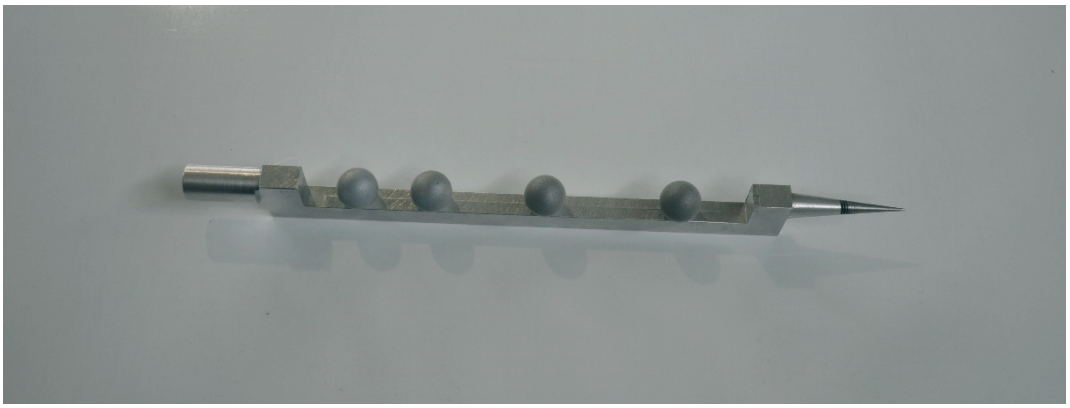

Fig. 6 Tentacle: calibration object with IR vision markers

each lever consists of two paired rods. The paired rods are continuously parallel during the operation of the machine. Because of this, tilting was disabled, so the mobile platform always moved in a plane parallel to the plane of the base platform. For simplicity, it can be assumed that the base platform was connected to the mobile platform via three arms. With known distances, the position of the tip of the tentacle was determined according to the CS of the mobile platform; in our case, it was located in the centre of the triangle by which it was geometrically defined. It is worth noting that, in the current design of the machine, the vectors from the centre to the corresponding vertices of the triangle of the base and mobile platforms of the machine are parallel during its operation, regardless of the position of the mobile platform. By monitoring the markers, the positions of all other joints on the machine can also be calculated.

IR reflective vision markers in the form of circular labels were placed on the stationary structural elements of the machine. After defining the zero point (the workpiece zero point) and the CS of the machine for the specified markers, the coordinates were determined. These markers were also used to find the transformation between the CS of the machine and that of the camera.

The procedure for finding the transformation between the 3D CS of the camera (within the vision system) and the CS of the machine starts with defining the origin of the machine CS [34-36].

The tip of the tentacle was placed on a given point whose coordinates were taken as the starting point for determining the positions of all points (Fig. 7). The tip of the tentacle was then brought to the remaining markers (their centres), and these positions were stored. Since the testing was performed on a machine based on parallel kinematics, the OCR readings of the values of the lever lengths were translated through the direct kinematics software module into the XYZ coordinates of the probe tip. In theory, three points are enough for the process of finding this transformation, but 25 points were used to get a more reliable result. These markers were also captured by the vision system and indexed, and their spatial positions were stored. Ultimately, there were two sets of paired 3D coordinates for the positions of one physical marker – those in the camera CS and those in the machine CS [34,37]. These sets were interrelated; for each point of the set in the camera CS, a correspondent point in the CS of the machine was known.

Fig. 7 The vision system follows the markers on the calibration object (tentacle) inserted in the machine tool holder

2.2.2 Defining the CS of the machine and establishing a relationship with the CS of the vision system

First, a relationship between the coordinate systems of the vision system and the machine is established. The transformation between the coordinate systems of the vision system and the machine and vice versa was calculated using numerical methods on the data that had been obtained. Since the obtained results (two 3D sets of points) also contained noise, the principal component analysis (PCA) was chosen to find the first solution of the transformation [38]. This transformation was iteratively improved by applying the nonlinear iterative closest point (ICP) algorithm [26]. The transformation that was obtained established the relationship between the coordinate systems of the camera and the machine, enabling visual monitoring of the movement of the mobile platform and a comparison of the position values with those read from the machine.

Based on the results from the previous steps, test programmes were formed. These enabled the movement of the mobile platform of the machine along given paths in the Cartesian coordinate system. These paths were translated by the software module for calculating inverse kinematics into desired lengths of the arms. When these lengths are achieved, the machine is in the wanted position. The movement of the mobile platform with a fixed tentacle was monitored by the vision system. In addition to the tentacles, a professional Optitrack vision system with a rated speed of 120 fps was used in the calibration procedure. This system enables the tracking of movements at higher rates and also allows an accuracy of 0.1 mm at distances of up to 2 m. A future project will include the construction of a professional vision kit based on commercially available hardware components to be used for this purpose. A prototype version of the kit has already been created. It is to be expected that the professional vision kit will produce similar results in tracking speed and will ensure sufficient accuracy at a significantly lower price. This approach enables the effective monitoring of important functions of the machine, the tracking of positions in near real-time, the finding of deviations from the given model, and the definition of the source of deviations. This creates the conditions in which shortcomings can be remedied and stability, appropriate speed, and reliability of operation ensured with the highest possible precision. The application of the vision system also enables continuous monitoring and the finding of errors in the operation of the machine in specific conditions that were not considered in the test phase of the evaluation of machine processes.

2.2.3 Calibration of A and C rotary axes

The application of the vision system that we created opens up the possibility of a simplified procedure for calibrating the machine and the rotary axes. If there are shortcomings, it is necessary to reduce them to the lowest possible level since even slight deviations create serious errors and unacceptable machining inaccuracies. This issue is primarily addressed in the construction and assembly of the machine. There are certain limitations in some designs due to imperfections in the design or the complex structure, which cause a significant problem in the implementation of the calibration procedure. In our prototype machine design, both issues were present; the application of the vision system is expected to be helpful and allow the calibration process to be carried out quickly and reliably.

After the physical establishment of coplanarity and orthogonality between the axes, additional calibration was performed using the vision system. The goal was to define the lines of the A and C rotary axes. The procedure involved placing a calibration object perpendicular to the A and C rotary axes. The calibration object was an aluminium or wooden bar with IR vision markers in the form of spheres, the centres of which were on the same line. Orthogonality between the line on which the markers were placed and the axis of rotation is not a requirement, but it is beneficial; the vision system had to allow the indexation of each marker. Thus, for an individual turn, each marker was tracked throughout the rotation. The procedure was performed following the calibration in which the origin of the machine coordinate system was defined, along with the transformation between the coordinate system of the machine and that of the vision system. This allowed the registered spatial positions of the markers to be shown in the machine CS. The capture was carried out in several turns.

The calibration object was then rotated and each angular step was recorded. As a result of each step, the spatial positions of individual markers rotated around the axis of rotation were obtained. This procedure was repeated for each turn and for a shift in the position of the calibration object along the observed axis. Finally, a set of spatial points was obtained for each turn; this set represents the circular path of each marker around the axis of rotation. Using numerical methods for the path of each marker, the centre of rotation was found. As a result, a set of points with small deviations in the distance from the axis of rotation was obtained (ideally, without deviation). This set was obtained for each turn, that is, it was captured with a calibration object placed at another location along the corresponding axis of rotation.

Using the least squares method [39], a spatially defined line was fitted through the centre points obtained from several turns conducted, where deviations from the points described above were minimised. If, according to the analysis, there were points that significantly deviated from the given line (outliers), they were excluded from further calculations, and the procedure was repeated without them. As a final result, the straight line that determines the axis of rotation in the CS of the machine was obtained. The same procedure was followed for the second axis. Thus, the A and C axes of rotation were defined.

3. Results and discussion

The aim of our study was to carry out the calibration of a 5-axis machine based on parallel kinematics using a vision system. The application of computer vision permitted practical and flexible implementation of the procedure. For this purpose, procedures were developed that enable:

- the calibration of the vision system to determine intrinsic and extrinsic parameters;
- the establishment of a relationship among the coordinate systems of the cameras;
- a 3D reconstruction of the positions of IR vision markers from multiple views;
- the use of an OCR module for character recognition on the computer display and the translation of the captured text into the required values;
- the use of a software module for capturing vision markers on the tentacle and determining the position of the tentacle tip;

- the establishment of a relationship between the coordinate systems of the machine and the vision system; and
- the calculation of the zero point of the machine and the definition of the A and C rotary axes of the machine.

In order to do this, appropriate hardware support was defined, obtained, and assembled, and the necessary software solutions were developed. To ensure adequate accuracy, each of these procedures was planned and carefully adopted.

The achievements related to the steps listed above are presented below.

3.1 The calibration of the vision system to determine intrinsic and extrinsic parameters

Zhang's procedure was used to calibrate the cameras and their relationship to the calibration object. This procedure enabled the calibration using planar objects with a binary (black and white) pattern in the form of a chessboard. For calibration purposes, the plate was rotated and captured with all the cameras. The number of images used was 70. In nine images (12.86%), the angles between the squares were not correctly detected, and these images were excluded from further processing. This phenomenon occurred in the images of the plates inclined towards the camera at 30 degrees or more. As a result, the calibration matrix $\boldsymbol{K}$ with intrinsic parameters, distortion factors, used in correcting the radial distortion of images, the $\boldsymbol{R}$ matrix, and the $\mathbf{t}$ vector (extrinsic factors) were obtained.

3.2 The establishment of a relationship among the coordinate systems of the cameras

A geometric relationship was established between the coordinate systems of all the cameras that synchronously captured the scene with the planar calibration object (chessboard) with known features. Using the P3P procedure, the spatial positions of the corners of the plate were found. During imaging, the vision system was stationary, as the panel was manually rotated on the platform. Ultimately, a cloud of points that were not in the same plane (coplanar) was obtained, along with their 2D positions in the image of each camera. This enabled the establishment of the relationship between each camera and the calibration object in the form of a cloud of 3D points. Since the imaging was synchronised and the image of the object in a certain position was taken from multiple views, this procedure allowed the relationships between the object and each camera to be established. In our case, from the 2D–3D correspondence, a metric projection matrix $\boldsymbol{P}$ (camera matrix) was calculated for each camera. This step, among other things, enabled the establishment of relationships between the cameras, which is a condition for the reconstruction of the spatial positions of points from their positions in the image.

3.3 3D reconstruction of the positions of IR vision markers from multiple views

The tracking of markers on the scene using multiple cameras and the reconstruction of their spatial positions and trajectories in the coordinate systems of arbitrarily selected cameras was carried out using intrinsic and extrinsic parameters from the calibration results and the image processing software for extracting the markers from the scene and finding their centres; the principles of epipolar geometry were used in the process. Professional Optitrack system cameras set to a capturing speed of 120 fps were used in our study. This system comes with software that allows the centres of markers to be tracked with an accuracy of +/– 0.1 mm at a distance of 2 m. Our goal was to create an affordable system. Optitrack was primarily used as the hardware to perform marker imaging, while the algorithms we developed were used to determine the position of the markers in space. Finally, the 3D reconstruction of the marker positions was also done using the Optitrack software, as a reference for comparing the results with those achieved by our procedures. The total deviation of the marker positions found by our algorithm from those found by the reference system was ~1.5%. This difference is expected to be reduced by further

improving the optimisation procedures. In this step, we achieved a technical solution in which the markers in the image were indexed, reconstructed, and tracked in their 3D positions.

3.4 The use of an OCR module for character recognition on the computer display and the translation of the captured text into the required values

The present control unit of the machine does not allow connection to external computers nor the reading of position values from the encoder on the linear axes of the machine. Since this problem is encountered in practice, a software solution was developed, which, in an unconventional way, allowed the required values to be read from the image of the captured screen of the control computer. By capturing a rectangular screen of known width and length, the relationship between its four corners on the physical model and those on the captured scene was established. These positions were located in the image of the screen that is projectively deformed. Since the screen is a planar object, it was possible to calculate the transformation by four correspondent points, which corrected the screen image and mapped it to a plane that was parallel to the one in which the screen model was located. This created an image of the screen, which was displayed as if it were taken in such a way that the optical axis of the camera was perpendicular to the plane in which it was located.

In this model, rectangular regions were selected according to the same pattern, and an individual parameter was read from each region. Of the several parameters that were read in our case, the most important for the current application were those concerning the current positions (lengths) of the three linear axes which, via levers, produce movements of the mobile platform with spindle and milling tools, but also those that show the angle of rotation for the A and C axes.

A smartphone camera was used to capture the screen of the control computer. The device was connected to the computer via Bluetooth protocol. The capturing was carried out at a speed of 4 fps, while the movements of the machine were temporarily paused when taking each individual image. The textual content and its numerical value were extracted from the defined regions in the screen image by an OCR module. After optimising the capturing parameters, adapting them to the conditions, and implementing several filters that improved thresholding and segmentation at the specified speed, 100% efficiency in the recognition of the positions of linear axes s and the angles of A and C axes was achieved. This result satisfied the conditions of our procedure and was utilised in the subsequent steps.

3.5 The use of a software module for capturing vision markers on the tentacle and determining the position of the tentacle tip

By using a unique design for the tentacle, a tool for the precise calibration of the machine was obtained. The tentacle described above was inserted into the spindle collet and clamped. There were four IR-reflective sphere-shaped markers on the tentacle in the known formation. They were illuminated during imaging from a source with IR diodes located on a disc around the camera lens. The centre of each marker was placed on the line that passes through the axis of the motor spindle and through the tip of the tentacle. The mutual distances between the centres of the markers, as well as from the markers to the tip of the tentacle, were known.

The procedure involved capturing the position of the tentacle, which moved in the work envelope of the machine. By reconstructing the positions of the marker centres, their 3D position in the CS of the selected camera was obtained. Also, using known 3D Euclidean distances between the individual markers and the condition of collinearity, the indexing of markers was obtained. It is sufficient to identify and index three markers to determine the direction in which each marker is located relative to another. From the known distances for an individual marker, its position was also defined. We tested the acceptability of the approach by placing a reflective IR marker in the form of a 0.2 mm thick circular sticker on a flat surface (Fig. 8). The spatial position of this marker in the camera CS was determined during recording. The tip of the tentacle was positioned on the marker in such a way that they came in contact without pressing. The tentacle

was then raised along the Z-axis by a known distance. The distance from the circular marker to the tip of the tentacle was measured with a calliper, and the result was compared. The average deviation calculated from 40 measurements was +/– 0.21 mm. Given that this was a prototype version of the machine and given the components used and the fact that there are many opportunities to improve the system, this result was adopted as adequate for use in the next steps.

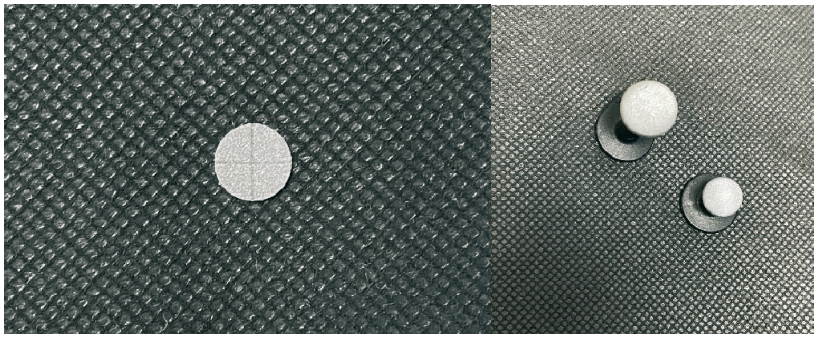

Fig. 8 The IR reflection dot and precision spheres on marker bases

3.6 The establishment of the relationship between the coordinate systems of the machine and the vision system

The procedure continued by establishing the relationship between the coordinate systems of the machine and the vision system. For this purpose, circular IR reflective markers in the form of stickers were placed in 25 positions on hard and fixed surfaces in the work envelope of the machine. The markers were placed in such a way that they were not in the same plane but were accessible to the tip of the tentacle. The centre of each marker had previously been discreetly marked in a way that did not compromise its position in the image. This subtle mark was used to bring the tip of the tentacle to that position. After positioning the tip of the tentacle at the centre of each marker, its position was read from the screen coordinates. Using the software solution for direct kinematics, we then calculated the XYZ position in the machine CS. In this position, the tentacle was also captured by the vision system and the XYZ position in its CS was obtained. As a result, two spatial point clouds were obtained. The procedure described above involves the transformation between the coordinate systems of the machine and the vision system. Testing showed that the results of this procedure were better when it was performed with a larger number of points. Also, more accurate results were achieved when the markers were placed at greater distances from each other. With the transformation and its inverse obtained, the coordinates of the points in the CS of the machine were read by the vision system and vice versa. This simplifies the calibration procedure of the machine, especially in the segment where it was not possible to reach individual points with the tentacle due to technical circumstances. A test programme was generated for testing purposes. The programme accomplished movements along a given path, which included a deviation from the (centrally) set starting point in the work envelope of the machine in the +/– X, Y, and Z directions. The movements were made in steps ranging from 20 mm up to 300 mm in each direction. For each step, the movement was paused, and the 3D position was read in the vision system CS and from the control computer screen, and then translated into an XYZ coordinate in the machine CS. By testing the obtained results, average position deviations of +/–0.35 mm were determined. This error was added to the error determined in the previous steps. Considering the circumstances described, the sources of the error, and the fact that there are numerous possibilities to upgrade the procedure, the result was accepted and the outcomes achieved in this step were employed in the subsequent procedure.

3.7 The calculation of the zero point and the definition of the A and C rotary axes of the machine

In this step, the machine parameters were calibrated, which is necessary for the creation of the software for generating paths. Based on the procedure described previously, the zero

point and the A and C rotary axes of the machine were determined. An aluminium bar was fixed in the A-axis clamping device. The second bar, with IR reflective spheres, was fixed transversely to it. This cross-connected structure allowed rotation around the axis and longitudinal movement of the transversely placed bar to an arbitrary position. The procedure involved tracking 12 IR markers that were put on the transversely laid bar (arm) that rotated around the axis for which the measurement was performed. Twenty rotations were performed, in which the arm was placed in 20 different positions along the axis for which the direction was calculated. In accordance with the technical characteristics of the machine and the design of the calibration object the A axis rotated in the range from 0 to 140 degrees, while the C axis rotated from -30 to +30 degrees in steps of 1 degree.

Every turn, in which the transverse axis was placed in a specific position, was captured, and the position in space of each marker was found. Each rotating point and its position are indexed. For this purpose the transverse bar with markers was linked to the bar that was fixed axially on the axis under consideration during the capture; the index was equal to the number of turns. The result obtained for each point in a set of points was the circular path of the point during rotation and the index was related to the position of the transverse profile. Each circular path consists of n spatial points that were part of a circle and were located in a plane perpendicular to the axis of rotation. The centre of the circumscribed circle of each marker was in the direction of the axis of rotation. The optimisation method provided the parameters of the circle, its spatial centre and radius, and the plane in which it was located. This procedure was performed for each tracked point (marker) and for all rotations. As a result, a cloud of points (centres of each circle) distributed around the axis of rotation was obtained.

This result was obtained using the principal component analysis (PCA) with iterative refining and the rejection of points with significant deviation. The procedure was performed separately for each rotary axis, resulting in two lines representing the A and C rotary axes. The point of intersection of the A and C axes was selected as the zero point. Given the imperfection of the machine prototype design, the zero point was chosen from among the points on the segment in which the distance between the two straight lines was smallest. The selection of this zero point caused an update of the transformation of the coordinate systems of the machine and the camera.

The results obtained were tested: the tests included placing a spherical IR marker at an arbitrary position on the bar transversely placed on the bar fixed to an axis of rotation. This marker was monitored by a stationary vision system with a known relation (transformation) to the machine CS. Since the axis of rotation (a line) was known in the CS of the machine, and so was its transformation into the CS of the vision system, there was an orthogonal projection of a given point (the centre of the marker) on it. In the subsequent step, the marker rotated around the selected axis by a known angle, and the vision system tracked its spatial position, which was also transformed into the machine CS. Ideally, the distance from the position of the marker centre to its projection would be the same for each rotation position. Also, with the known axis of rotation of the marker and the starting position, it was possible to calculate the position in space for each angle. This position should correspond to the position captured for this case by the vision system. Our results showed a mean deviation value of 0.81 mm, which is the difference between the expected and the measured value. In this step, the zero point of the machine was determined, and the A and C rotary axes were defined.

The calibration procedure for the machine was performed following the steps presented above. This procedure enables the creation of tool paths and the part machining. Essential software and algorithms were developed based on the available literature and the technical capabilities of the hardware used for capturing. The vision system was used to calibrate the prototype model of the machine based on parallel kinematics, and the whole vision system was based on consumer hardware. The fact that no professional components were used, except for the professional Optitrack system, mainly used as a reference system for testing algorithms, significantly raises the level of complexity; in addition, the measurement results are not as accurate as they would be if

professional components with better performance were used. Nevertheless, the achievements of the whole process confirmed the assumption that, even if only available hardware components and our own software are used, it is possible to achieve a sufficiently reliable vision system to calibrate the basic parameters of such a complex machine design.

There is room for improvement and error correction in every step. This system can be used for the calibration of most of numerical machining systems used in orthotics and prosthetics, regardless of whether they are conventional CNC machines or industrial robots, or whether they are used without technical documentation or are closed for external access. As a result of its peculiarities, our approach allows affordable components to be used. It is portable, scalable, and easy to calibrate and use. This solution, after upgrades, could be a helpful tool to speed up the implementation of numerical machining systems in O&P practice, and make it more economical. The results obtained are a good starting point. Calibration of the tool tip position will be described in an upcoming publication.

4. Conclusions

The presented machine is designed for making moulds for orthoses and related products in small orthotic and prosthetic practices. It is based on parallel kinematics and has five degrees of freedom. For its calibration, a vision system was developed. Taking into account the specifics of our problem, such as complex kinematics, a machine prototype, and the inability to connect to the control computer because of closed access, the vision system is designed to have special features for the quick and easy calibration of the machine and its adjustment, and, if necessary, for addressing other issues present. A prototype version of the system has been developed using the available hardware components, essential algorithms, and additional software support.

This system enables:

- Vision system calibration using precise, fast, simple, and cheap procedures;
- Monitoring of vision markers in the machine work envelope and reconstruction of their 3D positions and trajectories;
- OCR reading of the values of the positions of the machine linear axes from the screen of the machine control computer;
- Establishment of the relationship between the coordinate systems of the machine and the vision system; and
- Calibration of the zero point of the machine and the definition of the A and C axes of rotation.

The system was tested on the machine prototype, and the results obtained using the algorithms we had developed were compared with those obtained from the software of the reference vision system in the step related to the capture and reconstruction of the marker positions and paths. The results were also compared with the known values from calibration objects and with the known positions of the centre of the mobile platform and the tip of the tentacle perpendicular to the plane of the mobile platform; these were calculated from linear axis lengths and other parameters by using direct kinematics modules. An essential point in the consideration of the results is that the functionality and accuracy of each vision system depend entirely on a well-performed calibration procedure. The quality of the optics and the capabilities of the camera itself also have a significant influence. However, even if professional components are used but without a precise calibration procedure, such a system will not give satisfactory results in practice. Therefore, special attention is paid to this issue in our approach.

The results achieved indicate that the calibration of the vision system was carried out correctly and that it enabled the machine to be used in the further procedure. Deviations from the reference values were observed, but their size was acceptably small. In observing these deviations, their causes were identified and will be avoided through further improvements.

Following the calibration procedure, a vision system was created. It was used to record the scene, to extract IR vision markers, to define their positions in the camera CS, and to visualize their trajectories. A particular vision system also enabled a non-contact reading of the values of linear axis positions by capturing the screen of the control computer and extracting the values for each axis using the OCR method. Because of the previously mentioned technical limitations, this approach, which uses the module for direct kinematics, enables the XYZ positions of the centre of the mobile platform to be tracked in the CS of the machine.

When the probe is fixed in the collet on the spindle, the positions of the probe tip in the camera CS are captured by the vision system; given their XYZ coordinates in the camera CS, the coordinate systems of the machine and the vision system are related by a transformation. This enables the conversion of positions from the machine CS to the camera CS and vice versa. The advantage of this procedure is that it is possible to test algorithms, find positioning errors regardless of the cause, and compare the results obtained with two different methods.

This achievement enabled us to set the zero point (origin) of the machine and determine the directions of the A and C rotary axes. This enables the creation of settings on which the process of generating tool paths for a given geometry depends; in addition this enables constraints to be defined and a simulator to be achieved. The results of the tests done so far on the presented machine and the parameters obtained from the measurements using the vision system, meet the required accuracy condition (deviation of ≤ 2 mm) for making ankle foot orthosis moulds [40]. In the case of spinal orthoses, the tolerances are even less tight, so the machine in the existing form meets these needs.

Errors have been identified in all the procedures stated above. It was noticed that the errors accumulated through all the steps. A detailed analysis of errors is the subject of an ongoing process in which the observed hardware and software deficiencies will be corrected. After that, the process will be repeated, and all deviations should be significantly smaller. The results obtained so far indicate that, using the present hardware and an inexpensive vision system, it is possible to meet the needs of a calibration procedure of a machine with complex geometry and to adjust it to the required accuracy quickly, easily, and efficiently.

The application of the vision system in our approach has proved to be a helpful method to enable machine calibration, path generation, and simulation programme development, as well as simpler performance of other necessary actions. This fact is of special importance in practice when there is a requirement to adjust and parameterise a machine that has already been used, or the one with a unique kinematic design, or when there are restrictions on external access to settings. Such issues are common in the application of digital solutions in the manufacture of orthopaedic aids since manufacturers often decide to buy less expensive production systems that have these problems.

REFERENCES

[1] https://www.physio-pedia.com/Orthotics

[2] https://www.merriam-webster.com/dictionary/orthosis

[3] WHO standards for orthotics and prosthetics. *World Health Organization* 2017, ISBN 978-92-4-151248-0, https://apps.who.int/iris/bitstream/handle/10665/259209/9789241512480-part1-eng.pdf

[4] Barrios-Muriel, J.; Romero-Sánchez, F.; Alonso-Sánchez, F.J.; Rodríguez Salgado, D. Advances in Orthotic and Prosthetic Manufacturing: A Technology Review. *Materials* 2020, 13, 295. https://doi.org/10.3390/ma13020295

[5] Tiscareño, J.; Albajez, J.; Santolaria, J.. Analysis of different camera calibration methods on a camera-projector measuring system. *Procedia Manufacturing* 2019, 41, 539-546. https://doi.org/10.1016/j.promfg.2019.09.041

[6] Webster, J.; Murphy, D. Principles of Fabrication (Supan, TJ.) in *Atlas of Orthoses and Assistive Devices* (5th ed.), Elsevier Inc. 2017, 42-48. https://doi.org/10.1016/C2014-0-04193-7

[7] Farhan, M.; Wang, J.Z.; Bray, P.; Burns, J.; Cheng, T.L. Comparison of 3D scanning versus traditional methods of capturing foot and ankle morphology for the fabrication of orthoses: A systematic review, *Journal of Foot and Ankle Research* 2021, 14(1), 2. https://doi.org/10.1186/s13047-020-00442-8

[8] Obrovac, K.; Udiljak, T.; Mihoci, K. Foot orthosis design and manufacture. Transactions of FAMENA 2005, 29, 49-60.

[9] http://oandpnews.org/2012/07/09/prosthetics-113/

[10] Pandilov, Z.; Milecki, A.; Nowak, A.; Górski, F.; Grajewski, D.; Ciglar, D.; Mulc, T.; Klaić, M. Virtual Modelling and Simulation of a CNC Machine Feed Drive System, Transactions of FAMENA 2015, 39(4), 37-54.

[11] Smith, D.G; Burgess, E.M. The use of CAD/CAM technology in prosthetics and orthotics—Current clinical models and a view to the future. Journal of Rehabilitation Research and Development 2001, 38(3), 327–334.

[12] Gataš, B.; Pratikakis, I.; Perantonis, S.J. Adaptive degraded document image binarization. *Pattern Recognition* 2006, 39, 317-327. https://doi.org/10.1016/j.patcog.2005.09.010.

[13] Ashraf, N.; Arafat, S.; Iqbal, J. An analysis of optical character recognition (OCR) methods. *International Journal of Computational Linguistics Research* 2019, 10, 81. https://doi.org/10.6025/jcl/2019/10/3/81-91

[14] Sahu, N; Sonkusare, M. A study on optical character recognition techniques. *International Journal of Computational Science, Information Technology and Control Engineering* 2017, 4, 1-15. https://doi.org/10.5121/ijcsitce.2017.4101

[15] https://optitrack.com/cameras/v120-trio/

[16] Zhang, Z. A flexible new technique for camera calibration. *IEEE Transactions on Pattern Analysis and Machine Intelligence* 2000, 22(11) ,1330-1334. http://dx.doi.org/10.1109/34.888718

[17] Zhang, Z. Flexible camera calibration by viewing a plane from unknown orientations. *Proceedings of the Seventh IEEE International Conference on Computer Vision* 1999, 666–673. https://doi.org/10.1109/ICCV.1999.791289

[18] Burger, W. Zhang's camera calibration algorithm: In-depth tutorial and implementation. Technical Report HGB16-05. *Department of Digital Media, University of Applied Sciences Upper Austria* 2016, 1-56. https://doi.org/10.13140/RG.2.1.1166.1688/1

[19] Hödlmoser, M.; Zollner, H.; Kampel, M. An evaluation of camera calibration methods using digital low cost cameras. *Computer Vision Winter Workshop* 2010, Libor Špaček, Vojtčech Franc (Eds.), Nove Hrady, Czech Republic, February 3–5, *Czech Pattern Recognition Society*. 1-2. https://www.researchgate.net/publication/228774958_An_Evaluation_of_Camera_Calibration_Methods_Using_Digital_Low_Cost_Cameras

[20] Aldana, N.; Sandoval, L.; Hayet, J.-B.; Esteves, C.; Becerra, H.M. Coupling humanoid walking pattern generation and visual constraint feedback for pose-regulation and visual path-following. *Robotics and Autonomous Systems* 2020, 128, 7-8. https://doi.org/10.1016/j.robot.2020.103497

[21] Park, J.; Byun, S.-C.; Lee, B.-U. Lens distortion correction using ideal image coordinates. *Consumer Electronics, IEEE Transactions* 2009, 55, 987-991. https://doi.org/10.1109/TCE.2009.5278053

[22] https://homepages.inf.ed.ac.uk/rbf/CVonline/LOCAL_COPIES/EPSRC_SSAZ/node3.html

[23] https://www.cs.cmu.edu/~16385/s17/Slides/11.1_Camera_matrix.pdf

[24] Xiao, X.L.U. A review of solutions for perspective-n-point problem in camera pose estimation, *First International Conference on Advanced Algorithms and Control Engineering, IOP Conf. Series: Journal of Physics: Conf. Series* 1087 2018, 3-6. https://doi.org/10.1088/1742-6596/1087/5/052009

[25] https://www.ipb.uni-bonn.de/html/teaching/msr2-2020/sse2-13-DLT.pdf

[26] Tian, H.Q.; Dang, X.Q.; Wang, J.H.; Wu, D.M. Registration method for three-dimensional point cloud in rough and fine registrations based on principal component analysis and iterative closest point algorithm. *Traitement du Signal* 2017, 34(1-2), 57-75. https://doi.org/10.3166/TS.34.57-75

[27] Hartley, R.; Zisserman, A. *Multiple view geometry in computer vision* (2nd ed.). Cambridge University Press 2004.

[28] Cyganek, B.; Siebert, J.P. *An introduction to 3D computer vision techniques and algorithms*. John Wiley & Sons, Ltd 2009. https://doi.org/10.1002/9780470699720

[29] https://en.wikipedia.org/wiki/Fundamental_matrix_(computer_vision)

[30] Luong, Q.T.; Faugeras, O.D. Self-calibration of a moving camera from point correspondences and fundamental matrices. *International Journal of Computer Vision* 1997, 22, 261-289. https://doi.org/10.1023/A:1007982716991

[31] Morė, J.J. The Levenberg-Marquardt algorithm: Implementation and theory, in G. A. Watson (Ed.) *Numerical Analysis* (pp. 105-116) Springer, 1977. https://www.osti.gov/servlets/purl/7256021. https://doi.org/10.1007/BFb0067700

[32] http://www.nct.hu

[33] https://en.wikipedia.org/wiki/Tesseract_(software)

[34] Šuligoj, F.; Jerbić, B.; Šekoranja., B; Vidaković, J.; Švaco, M. Influence of the Localization Strategy on the Accuracy of a Neurosurgical Robot System. Transactions of FAMENA 2018, 42(2), 27–38. https://doi.org/10.21278/TOF.42203

[35] Xiang, T.; Yi, J.; Li, W. Five-Axis Numerical Control Machining of the Tooth Flank of a Logarithmic Spiral Bevel Gear Pinion. Transactions of FAMENA 2018, 42(1), 73-84. https://doi.org/10.21278/TOF.42203

[36] Wu, Y.; Hou, L..; Ma, D.Q.; Wei, Y.; Luo, L. Milling Machine Error Modelling and Analysis in the Machining of Circular-Arc-Tooth-Trace Cylindrical Gears[J]. Transactions of FAMENA 2020, 44(4), 13-29. https://doi.org/10.21278/TOF.444009419

[37] Šekoranja, B.; Jerbić, B.; Šuligoj, F. Virtual surface for human-robot interaction. Transactions of FAMENA 2015, 39, 53-64.

[38] https://www.cs.princeton.edu/picasso/mats/PCA-Tutorial-Intuition_jp.pdf

[39] https://www.ltu.se/cms_fs/1.51590!/svd-fitting.pdf

[40] Schrank, E.S.; Stanhope, S.J. Dimensional accuracy of ankle-foot orthoses constructed by rapid customization and manufacturing framework. *Journal of Rehabilitation Research & Development* 2011, 48, 1, 31-42. https://doi.org/10.1682/JRRD.2009.12.0195

ABBREVIATIONS

CNC	Computer Numerical Control	O&P	Orthotics and Prosthetics
CAD	Computer-Aided Design	CAM	Computer-Aided Manufacturing
OCR	Optical Character Recognition	CS	Coordinate System
HW	Hardware	fps	frames per second
QR decomposition	(also known as QR factorization) is decomposition of matrix into matrices [Q] (orthogonal matrix) and matrix [R] (upper triangular matrix)		
PCA	Principal Component Analysis is the process of computing the principal components and using them to perform a change of basis on the data. It is often used to reduce the dimensionality of large data sets.		
ICP	Iterative Closest Point is an algorithm employed to minimize the difference between two clouds of points.		

Submitted: 16.02.2022

Accepted: 20.7.2022

Josip Nižetić
Cognitus d.o.o, Zagreb, Croatia

Pero Raos
Goran Šimunović
University of Slavonski Brod, Mechanical Engineering Faculty, Slavonski Brod, Croatia

Miho Klaić
University of Zagreb, Faculty of Mechanical Engineering and Naval Architecture, Zagreb, Croatia

Alan Mutka
Rochester Institute of Technology Croatia, Zagreb, Croatia

*Corresponding author:
josip.nizetic@cognitus.hr